Computer Vision Winter Workshop 2010, Libor Špaček, Vojtěch Franc (eds.)
Nové Hrady, Czech Republic, February 3–5
Czech Pattern Recognition Society

Range Image Registration of Specular Objects

Diego Thomas and Akihiro Sugimoto

National Institute of informatics, Japan
diego_thomas@nii.ac.jp, sugimoto@nii.ac.jp

Abstract *We present a method for range image registration of specular objects devoid of salient geometric properties under complex lighting environment. We propose to use illumination consistency on two range images to detect specular highlights, which are used to obtain diffuse reflection components. By using light information estimated from the specular highlights and the diffuse reflection components, we extract photometric features invariant to changes in pose and illumination, even under unknown complex lighting environment. We then robustly register the two range images using these features. This technique can handle various kind of illumination situations and can be applied to a wide range of materials. Our experiments using synthetic data show the effectiveness, the robustness and the accuracy of our proposed method.*

1 Introduction

Detailed modeling of real objects in controlled or uncontrolled environments has been of crucial interest in the past decade. When creating a 3D model of a real object using laser range scanners, multiple range images of the same object are captured at different poses from a fixed viewpoint. Because each range image is represented in the local coordinate system depending on the position and pose of the sensor, the transformations aligning all images have to be computed. This process is called range image registration.

In this paper we will focus on range image registration of a non-Lambertian textured object devoid of salient geometric features under uncontrolled environment. We assume that two range images are captured from two different poses, with a fixed viewpoint and fixed unknown illumination conditions.

The irradiance at a point on an object surface changes when the object pose changes. As a consequence, the photometric appearance, such as color, of the same point in different range images changes. Using photometric features that depend on the object pose thus degrades the performance of the registration when they are used for establishing matchings.

Albedo of the object surface is invariant to the object pose, viewpoint or illumination conditions. This property depends on only the object material and exhibits sufficient saliency for matching in the case of textured surfaces. Therefore, albedo is a powerful feature for range image registration of textured objects devoid of salient geometric features under fixed illumination conditions.

Albedo at a point is the ratio of the diffuse reflected light over the irradiance. It can be directly computed when both the diffuse reflection and the incident illumination at this point are known. However, under uncontrolled environments or if the surface exhibits specular reflections (like shiny objects for example), computing albedo becomes a demanding problem. As a consequence, existing methods that make use of albedo, for example [4, 17], assume the Lambertian surface (diffuse reflection only) and known incident illumination. In these approaches, the specular reflections at the surface of an object are not considered.

We propose a method for registering two range images of a specular object under unknown illumination environment. To compute albedo at the surface, incident illumination and diffuse reflection components are required. For each range image, we generate candidates of light source directions, using normals at the surface and local peak of intensity. Illumination consistency on two range images allows us to select light source directions among the candidates. The detected light source directions then enable us to define regions where the reflection components are accurately separated. We compute albedo in these regions and extrapolate it by using neighboring similarities. In this way, we obtain albedo over the range images. The albedo is used as an input of an existing registration algorithm to show the usefulness of our proposed method. Our intensive experiments show the effectiveness of our proposed method. To our best knowledge, no method on range image registration has been proposed that can handle specular objects under unknown illumination environment.

2 Related works

For objects lacking in salient geometric features, many approaches using photometric features have been discussed. For example, Godin *et al.* [5] proposed to use dense attributes of range image elements as a matching constraint. Weik [19] proposed to use texture intensity gradient and intensity difference. Johnson and Kang [6] proposed to deal with textured 3D shapes by using color. Okatani *et al.* [12] proposed to use chromaticity for registration. Brusco *et al.* [3] proposed to incorporate texture information in the concept of spin-images. Pulli *et al.* [13] proposed a new mismatch error to improve registration using both color and geometric information. However, because color or chromaticity depends on the object pose, the viewpoint

and illumination, the performance of these methods is degraded when the illumination change has significant effects on the object appearance.

On the other hand, albedo is a photometric property invariant to the pose of the object, the illumination condition and the viewpoint, and is thus powerful for the purpose of matching. Cerman *et al.* [4] proposed to use albedo difference to match points for range image registration. However, this point-based approach is sensitive to data noise and requires precise knowledge on the illumination. Therefore it is not practically applicable to real data.

More recently Thomas *et al.* [17] proposed to use local distribution of albedo to enhance robustness for range image registration. Adaptive regions are defined at the surface of an object by using local distribution of albedo and a metric is then defined to match points using the regions. The rigidity constraint on surface is also introduced to eliminate false matches to improve accuracy of matching. Though this method achieves robust registration under a rough estimation of illumination, it is limited to Lambertian objects illuminated by a single distant light source.

In other approaches, Bay *et al.* [1] proposed a scale and rotation invariant descriptor called SURF that makes use of an integral image to speed up the computation and comparisons. Tola *et al.* [18] also proposed a local descriptor that can be quickly computed and used even in low-quality images. However, these approaches are more focused on computational efficiency rather than accuracy.

To deal with specular reflections under complex illumination environments, recent works on reflectance analysis can be used. Several methods to separate or decompose reflection components of textured surfaces can be found in the literature ([10], [14], [8]). For example, Lin *et al.* [8] proposed to separate reflection components from a sequence of images by computing the median intensity of corresponding pixels in the image sequence. However, this method requires a large number of images as well as pixel correspondences between all images. It is thus inappropriate for range image registration.

Tan *et al.* [15] proposed a method to separate reflection components of textured surfaces from a single image. By assuming the dichromatic reflection and a single distant light source, a specular free image is generated by locally and non-linearly shifting each pixel's intensity and maximum chromaticity. This specular free image has exactly the same geometrical profile as the diffuse components. Though this method achieves accurate separation of reflection components, it can not handle multiple light sources and high intensity textures.

In contrast to previous work, our proposed method can handle changes in photometric appearance, non-Lambertian surfaces and unknown complex illumination environments even in the presence of high intensity textures.

3 Overview of the proposed method

Our approach can be decomposed into two parts. We first locally compute albedo in some regions of the surface of the object by using the input color images, normals and illumination consistency. The second uses neighboring similarities of the input color images to extrapolate local albedo into the rest of the surface. The obtained albedo is then used as an input of an existing ICP-like [2] robust framework to estimate the transformation aligning two range images [17]. Fig. 1 illustrates the flow chart of our proposed method.

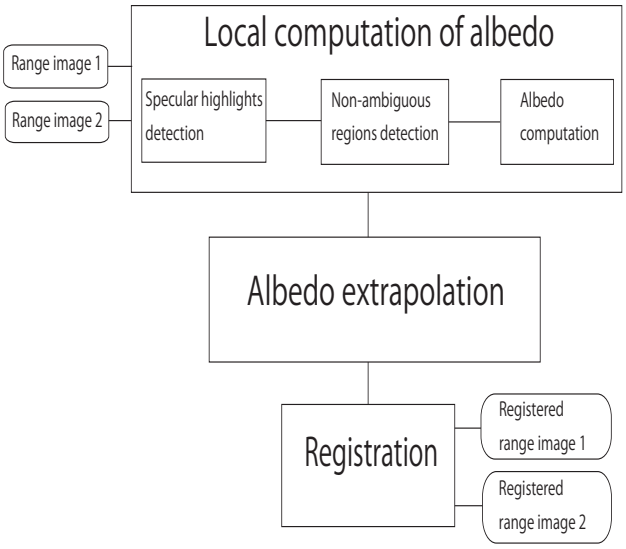

Figure 1: Basic flow of the proposed method.

Local computation of albedo Computing albedo in the presence of specular reflection under unknown illumination environment is a demanding problem. Recent works on reflectance analysis allow us to separate reflection components of the surface using the dichromatic reflection model and thus to retrieve the diffuse reflection component, under the assumption of a single distant light source and without high intensity textures. To deal with complex illumination environment (multiple light sources), we propose to separate the reflection components of the surface only inside sub-regions where the local illumination can be approximated by a single distant light source (in this paper we will call such regions non-ambiguous regions in contrast to the rest of the surface that is referred to as ambiguous region). We use local peaks of intensity and normals at the surface to estimate possible light source directions and we use the illumination consistency to eliminate false detections. We then define regions where the reflection components can be separated, and use the separated diffuse reflection component together with the estimated light source directions to compute albedo in these regions.

Extrapolation of albedo into ambiguous regions It is not possible to directly compute albedo in ambiguous regions because these regions are significantly affected by multiple light sources, and thus points in these regions can not be directly used for matching. However, albedo in non-ambiguous regions has been computed and it is to

be expected that several points in the ambiguous region have albedo similar to points in non-ambiguous regions. We thus extrapolate albedo computed in non-ambiguous regions to the rest of the surface. By considering a small region at the surface and under the assumption of a smooth surface, the irradiance changes are relatively small and thus by comparing maximum chromaticity we are able to detect points with similar albedo.

4 Local computation of albedo

Computing albedo at the surface requires the diffuse reflection components and the light source directions. In the case of a scene illuminated by a single distant light source and given the corresponding illumination chromaticity, a method exists that separates the reflection components of the textured surface [15]. On the other hand, in our case, the illumination environment is not restricted to a single light source and such a separation technique can not be applied to the whole surface. However, even in the case of multiple light sources, there exist some regions where the incident illumination can be approximated by a single light source. We thus divide the whole image into regions so that we have a region illuminated by a single light source. We can then separate the reflection components of the region to locally compute albedo.

For each region specified above, the incident illumination is approximated by a single light source. To separate the reflection components in this region, the corresponding illumination chromaticity is required. To compute illumination chromaticity, several methods based on color constancy can be found in the literature ([16], [7] for example). In particular, the method [16] achieves robustness as well as accurate estimation of the illumination chromaticity by using specular reflection intensity. However, this method does not account for high intensity texture regions that may appear like specular highlights and that would degrade the estimation of the illumination chromaticity. We employ illumination consistency to discriminate between specular highlights and high intensity texture regions. Light source directions are then selected accordingly.

4.1 Detection of specular highlights

To define a region where the incident illumination can be approximated by a single light source, a light source direction is required. For a smooth surface, a specular highlight is centered on the mirror-like reflection direction, which is useful to estimate incident illumination direction. Moreover, as proposed in [16], we estimate the illumination chromaticity by using specular reflection intensity. As a consequence, detecting the specular highlights at the surface is of major importance. If the surface exhibits regions with high intensity texture, it becomes difficult to distinguish between specular highlights and regions with high intensity texture. Therefore, we first detect all highlights at the surface that can be either a specular highlight or a high intensity texture region. We then employ illumination consistency between two range images to discriminate specular highlights from high intensity texture regions.

Highlight detection If we consider a region with homogeneous texture, then a specular highlight will exhibit a local peak of intensity. This is because the specular reflection component increases as the viewing direction comes closer to the mirror-like reflection direction. We thus detect local peaks of intensities at the surface. Points with lowest intensities in the image are first removed to focus on only significant specular highlights (with sufficient intensity). Then we obtain several connected regions. For each connected region, the average avg and standard deviation std of the intensities are computed and each pixel $\mathbf{x}$ such that $\mathbf{I}(\mathbf{x}) > avg + std$ is selected, where $\mathbf{I}(\mathbf{x})$ is the intensity at $\mathbf{x}$. Then, if the initial connected region is separated into several connected parts the process is iterated. The detection stops when the number of connected regions becomes stable. Each connected region represents one possible specular highlight.

Specular highlights Some of the detected highlights may be high intensity texture regions, which may cause inaccurate estimation of the illumination chromaticity as well as inaccurate estimation of incident illumination directions. This is because the surface may exhibit high intensity texture regions that behave like a specular highlight. We thus employ illumination consistency to discriminate between specular highlights and high intensity texture regions.

The illumination condition is the same for two range images. This means that the light source directions producing corresponding specular highlights are the same. We will call this illumination consistency below. Because normals at the surface are available for two range images, for each highlight in two range images, we estimate the incident illumination direction that can produce such highlight. To be more specific, we first compute the average of the viewing directions in the highlight region and then rotate this vector around the averaged normal vector with an angle equal to $\frac{\pi}{2}$ to estimate the incident light vector. This is because for smooth surfaces, the viewing directions in this region is roughly centered on the mirror-like specular reflection direction.

The highlight regions are then clustered into groups that are produced by similar light sources. Namely, consider the sets $(H_{1,j})_{j\in[0,n_1]}$ and $(H_{2,j})_{j\in[0,n2]}$ of the highlight regions of two range images, with n_1 and n_2 the number of highlight regions. We regroup highlight regions using the criterion below:

$$\forall i \in [1,2], \forall (j,j') \in [0,n_i], \text{ if } \mathrm{acos}(\mathbf{l}_{\mathrm{i,j}} \cdot \mathbf{l}_{\mathrm{i,j'}}) < \mathrm{Th_l} \\ \text{then the corresponding regions are regouped,} \quad (1)$$

where $\mathbf{l}_{i,j}$ is the estimated normalized light direction for the highlight region $H_{i,j}$, $(\mathbf{l} \cdot \mathbf{l}')$ is the scalar product of two vectors $\mathbf{l}$ and $\mathbf{l}'$ and Th_l is a threshold (for example 20 degrees). When two regions $H_{i,j}$ and $H_{i,j'}$ are regrouped, $H_{i,j'}$ is added to $H_{i.j}$, $l_{i,j} = \frac{l_{i,j}+l_{i,j'}}{2}$and $H_{i,j'}$ is removed from the list of highlight regions.

We then eliminate high intensity texture regions using the illumination consistency constraint. Namely, we use the

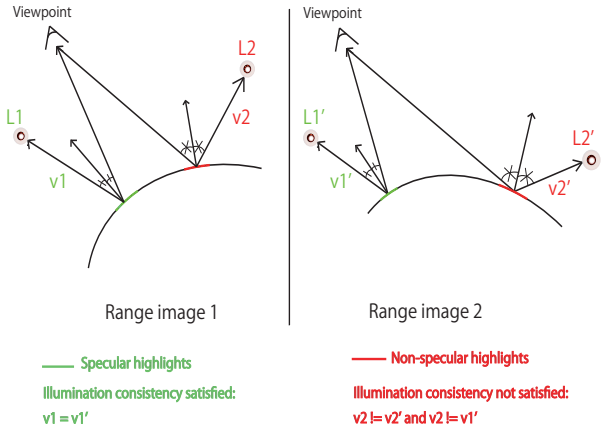

Figure 2: Illumination consistency constraint.

criterion below:

$$\begin{aligned} &\forall i \in [1,2], \forall j \in [0, n_i], \\ &\text{if for i}' \in [1,2], \text{i}' \neq \text{i}, \forall \text{j}' \in [0, \text{n}_{\text{i}'}], \\ &\qquad \text{acos}(\mathbf{l}_{\text{i,j}} \cdot \mathbf{l}_{\text{i}',\text{j}'}) > \text{Th}_\text{l}, \\ &\text{then the region } H_{i,j} \text{is eliminated.} \end{aligned} \tag{2}$$

Fig. 2 illustrates the illumination consistency constraint under a fixed viewpoint and fixed illumination condition.

We finally obtain consistent specular highlights on two range images with their estimated incident light direction. These specular highlights are then used to compute the illumination chromaticity of each light source. The estimated light source direction are used to divide the image into regions each of which is mostly illuminated by a single dominant light source.

4.2 Detection of non-ambiguous regions

For each specular highlight, we have estimated its mostly dominant light source direction. If the incident illumination of a region is a single distant light source, we can use the method [15]. We can not directly apply the method [15] to the whole surface. This is because the illumination environment can be composed of multiple light sources. In fact, this method requires a normalized image that simulates pure white illumination. However, the normalization process is not additive, not even linear and thus this is impossible to obtain if the scene is illuminated by unknown multiple light sources with different colors. Each light source illuminating the scene has different positions and accordingly the energy emitted at a point from each light source is different. This means that the surface exhibits regions where the incident illumination can be approximated by a single light source. We thus divide the surface into sub-regions, so that non-ambiguous regions are specified where the local incident illumination can be approximated by a single distant light source.

We assume that each detected light source is distant from the surface so that the incident light rays coming from one light source is the same for all points at the surface. By using the detected incident light directions we compute a shadow map for each detected light source. Namely, for

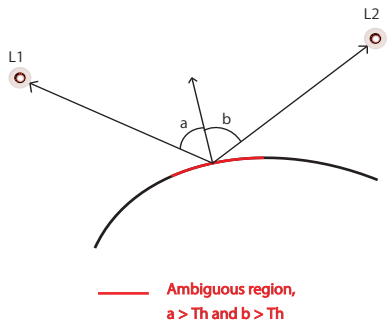

Figure 3: Definition of ambiguous regions.

a light L with directional vector $\mathbf{l} = (l_x, l_y, l_z)$, we define the shadow map S induced by L proportional to the energy received from L by each point at the surface. More precisely, for a point $\mathbf{x}$ on the surface with normal $\mathbf{n}$ and with angle Θ between $\mathbf{l}$ and $\mathbf{n}$ we define

$$S(\mathbf{x}, L) = \cos\Theta. \tag{3}$$

To detect non-ambiguous regions, we use the criterion below:

$$\begin{aligned} &\text{if } (S(\mathbf{x}, L_1) > Th_\alpha \text{ and } S(\mathbf{x}, L_2) > Th_\alpha) \\ &\qquad \text{then } \mathbf{x} \text{ is in an ambiguous region} \\ &\qquad \text{else } \mathbf{x} \text{ is in a non-ambiguous region,} \end{aligned} \tag{4}$$

where L_1 and L_2 are the two light sources such that the intensities of the shadow maps at the point $\mathbf{x}$ are the greatest. The threshold Th_α is a value between 0 and 1. In the experiments, we chose $Th_\alpha = 0.7$ that corresponds to an angle Θ of about 45 degrees. For each non-ambiguous regions, we attach the light source that emits the most energy inside this region and regroup regions with the same corresponding light sources. We remark that it is preferable to over-detect ambiguous regions rather than non-ambiguous regions. This is because high errors in the albedo estimations may propagate during the subsequent extrapolation process.

As a consequence, we obtain non-ambiguous regions in two range images in which we can reliably and adaptively separate reflection components using a single distant light source.

4.3 Estimating albedo

The energy emitted from a specular highlight to the viewpoint comes mainly from a single light source. Each light source induces a specular highlight at the surface, which allows us to compute its illumination chromaticity, and each non-ambiguous region has its corresponding light source. As a consequence, for each non-ambiguous region the incident illumination can be approximated by a distant single light source whose illumination chromaticity can be computed. We can thus independently apply the method proposed in [15] to each non-ambiguous regions for separating the reflection components of these parts of the surface. We briefly recall the method proposed in [15].

The dichromatic reflection model at a pixel $\mathbf{x}$ can be expressed as:

$$\mathbf{I}(\mathbf{x}) = \omega_d(\mathbf{x})\mathbf{B}(\mathbf{x}) + \omega_s\mathbf{G}, \tag{5}$$

where $\mathbf{I} = (I_r, I_g, I_b)$ is the color vector of image intensity, $\mathbf{x} = (x, y)$ is the image coordinate, $\omega_d(\mathbf{x})$ and $\omega_s(\mathbf{x})$ are the weighting factors for diffuse and specular reflections, $\mathbf{B}(\mathbf{x})$ represents the color vector of diffuse reflection and $\mathbf{G}$ represents the color vector of the specular reflection. Note that we assume that the specular reflection intensity is equal to the illumination intensity, without any inter-reflections. The first part of the right-hand side of the equation represents the diffuse reflection component and the second part represents the specular reflection component. The basic idea is to iteratively compare the intensity logarithmic differentiation of an input image and its specular-free image. We remark that a specular-free image is an image that have exactly the same profile as the diffuse image.

The input image should be a normalized image that simulate a pure white illumination. To do so, the input image is normalized by the illumination chromaticity, which is computed from the specular highlights using the method proposed in [16]. The specular-free image is generated by shifting each pixel's intensity and maximum chromaticity nonlinearly. Given a normalized and a specular-free image, the reflection components are then iteratively separated until the normalized image has only diffuse pixels.

As a result a diffuse normalized image is obtained. This estimated diffuse image is then used, together with the estimated light source direction corresponding to the non-ambiguous region and the diffuse reflection model to estimate albedo in this region.

5 Extrapolation of albedo

Up to here, we have computed albedo in non-ambiguous regions. However, in ambiguous regions, albedo is still unknown and matching points in these regions is not yet possible. We remark that albedo has been computed in several parts of the surface and it is to be expected that several points in the ambiguous region have albedo similar to points in non-ambiguous regions. We thus estimate albedo in the ambiguous region by extrapolating albedo computed in non-ambiguous regions.

We consider a small region at the surface without specular highlights. The energy reflected at points inside this region is then mostly diffuse. As a consequence, the chromaticity or maximum chromaticity of points inside this small region with the same surface color is similar to each other. Therefore, by comparing maximum chromaticity of points inside small regions we can detect points having similar albedo.

For a point $\mathbf{x}$ at the surface, the maximum chromaticity $\sigma(\mathbf{x})$ of the point $\mathbf{x}$ is defined as follows:

$$\sigma(\mathbf{x}) = \frac{\max(I_r(\mathbf{x}), I_g(\mathbf{x}), I_b(\mathbf{x}))}{I_r(\mathbf{x}) + I_g(\mathbf{x}) + I_b(\mathbf{x})}. \tag{6}$$

Starting from the diffuse points in the ambiguous region that have a neighbor in a non-ambiguous region, albedo values are iteratively and locally extrapolated until the size of the ambiguous region converges to a constant value. At each iteration, considering a point $\mathbf{x}$ at the border of the ambiguous region, we extract the point $\mathbf{y}$ in the vicinity of $\mathbf{x}$ such that $\epsilon = |\sigma(\mathbf{x}) - \sigma(\mathbf{y})|$ is minimal and albedo of $\mathbf{y}$ is known. If ϵ is smaller than a threshold Th_ϵ (for example $Th_\epsilon = 0.1$) then we set the albedo value of $\mathbf{x}$ to the one of $\mathbf{y}$ and remove $\mathbf{x}$ from the ambiguous region. Namely, we process as follows:

$$\begin{aligned} \mathbf{y} = \text{argmin}_{\mathbf{p}\in V(\mathbf{x})}(|\sigma(\mathbf{x}) - \sigma(\mathbf{p})|), \\ \text{if } |\sigma(\mathbf{x}) - \sigma(\mathbf{y})| < Th_\epsilon, \\ \text{then } alb(\mathbf{x}) = alb(\mathbf{y}) \\ \text{and we remove } \mathbf{x} \text{ from the ambiguous region,} \end{aligned} \tag{7}$$

where $alb(\mathbf{x})$ is the albedo of point $\mathbf{x}$ and $V(\mathbf{x})$ is a vicinity of $\mathbf{x}$ such that $\forall \mathbf{p} \in V(\mathbf{x}), \|\mathbf{x} - \mathbf{p}\|_2 < Th_V$ and $\mathbf{p}$ is in a non-ambiguous region, with Th_V a threshold (for example $Th_V = 0.06$ mm if the resolution of range image is 0.01 mm). Fig. 4 illustrates different stages of the extrapolation procedure.

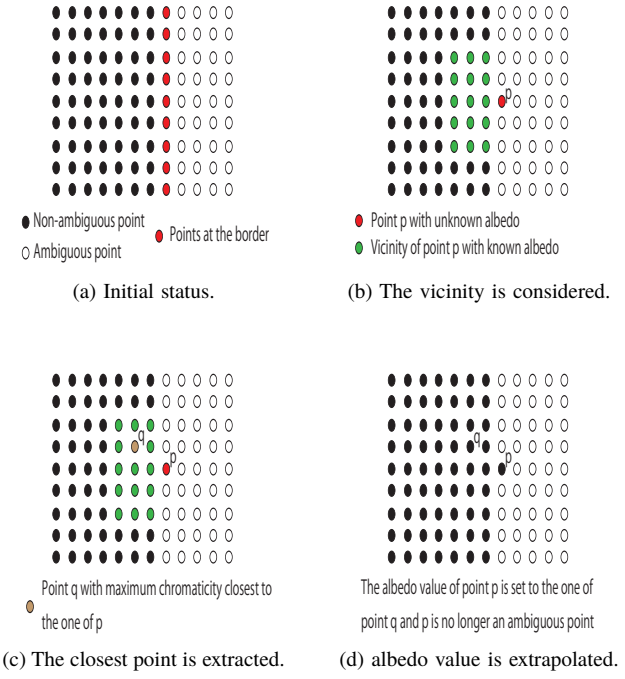

(a) Initial status. (b) The vicinity is considered.

(c) The closest point is extracted. (d) albedo value is extrapolated.

Figure 4: The different stages for the extrapolation.

As a result we extrapolate albedo to the rest of points at the surface that are not inside a specular highlight. We then obtain photometric features that are globally invariant to the pose of the object, the viewpoint and illumination conditions. These features are thus useful for registering range images. The obtained range image where each point has its corresponding albedo is called the albedo map.

6 Registration

In order to show the usefulness of our method, we use our estimated albedo map as an input of the iterative method for range image registration proposed in [17].

The method [17] uses adaptive regions defined from the local distribution of albedo. Namely, by defining a speed image for a range image, from each point a contour is propagated using a level-set approach, which defines an adapted region for each point.

A similarity metric between two points of interest is then defined based on supports from the corresponding points inside regions for the two points. This similarity metric represents the albedo similarity of corresponding points inside the regions weighted by the geometric similarity of the regions. To eliminate incorrect matches the rigidity constraint is used.

As a result, the obtained list of matches is robust and accurate enough to be used for the estimation of the transformation using a weighted least square approach [9].

7 Experiments

We conducted experiments with synthetic data to verify the robustness of our proposed method against changes in illumination conditions, surface properties and noise in both normals and intensities. The synthetic data were obtained with a 3D modeler software (3D Studio Max) (see Table 1). The exact albedo image is known and we simulated intensity at the surface with a known specular reflection component and synthetic light sources using the Torrance and Sparrow reflection model [11] (Fig. 5).

In order to see the effects against data noise we randomly transformed the normals and intensity of the two range images. More precisely, the normals were first rotated around an arbitrary axis orthonormal to the ground truth normal with an angle α. Then the rotated normal is rotated around the ground truth normal with a random angle θ with value ranging from 0 degrees to 360 degrees. On the other hand, the surface intensity was perturbed with Gaussian noise with 0 mean and λ variance, where λ is a percentage of the average over the ground truth intensity of the surface.

In order to see the effects against illumination conditions. We rendered two images with various kinds of illumination. The light source direction is computed using the normal at a point $\mathbf{x}$ and the viewpoint, and the light source position is defined at an arbitrary distance on the light direction. This is because we need specular highlights at the surface to test our method. Rather than choosing the position of the light source randomly we preferred to choose a random point $\mathbf{x}$ at the surface that represents the perfect specular reflection from the viewpoint.

Before applying our method, we manually established a rough pre-alignment of two range images. This alignment allowed us to simulate the case where the input data were captured from two different viewpoints rotationally differentiated by 18.09 degrees around the axis $(0.0057, 0.9997, -0.025)$.

We evaluated our method with different values of α and λ. The value α was changed from 0 to 54 degrees by 2.86 degrees. The value λ was changed from 0 to 9 percents by 0.5 percents. For each values of α, λ, we applied our method 20 times under the same initial conditions.

Table 1: Description of the synthetic data.

Nb_Points	Resolution	Expected_rot (angle; axis)
30650	0.01mm	$(18.09; 0.0057, 0.9997, -0.025)$

(a) Superimposed range image. (b) First image. (c) Second image.

Figure 5: The input synthetic data.

Fig. 6 shows quantitative evaluation of registration results in terms of averages and variances of the angle error and axis error of the obtained results under various different level of noise in both normals and in intensity. Our method achieves robustness for both noise in normals and intensity. We observe that even with a noise in intensity of variance 8% the largest error remains under 0.8 degrees for the angle accuracy and under 2.5 degrees for the axis accuracy. For noise in normals, we observe that even with a noise of variance 10 degrees, the largest error remains under 0.2 degrees for the angle accuracy and under 1 degree for the axis accuracy. Fig. 8 shows an example of the estimated photometric features computed for the input range images in Fig. 5 and the qualitative result of the registration. In this example, we obtained an angle error of 0.07 degrees and an axis error of 0.06 degrees. The resolution of this data is about 0.01mm and its depth is about 0.5mm, therefore the transformation error corresponds to a distance error between the obtained and the ground truth position of points of approximately 0.09mm. We thus observe that the registration achieves accuracy of the same precision of the acquisition device accuracy. We also observe that as expected the specular effects are correctly removed and that the features are globally invariant to the viewpoint, the pose of the object and the illumination. As we expect, the obtained photometric features are consistent for the two range images.

In order to test the accuracy of our method under complex illumination conditions, we changed the position between the specular highlights that define the light source directions. One light was fixed and considered as a reference light. We then evaluated our method with three different values of d, where d is the distance of two different specular highlights: 1.8, 1.2 and 0.8. For each value of d the method was applied 20 times with a random light direction. Table 2 shows the results obtained with our method. The value $Ratio$ is the ratio of ambiguous points over the total number of points in the two range images. We ob-

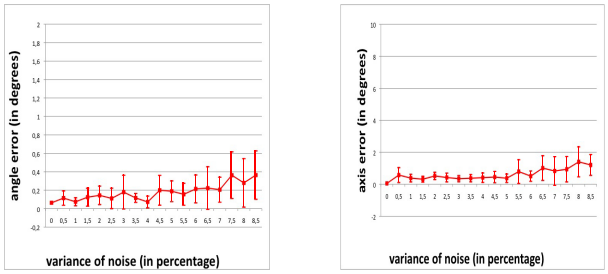

(a) Angle error. (b) Axis error.

Figure 6: Results under noise in intensities.

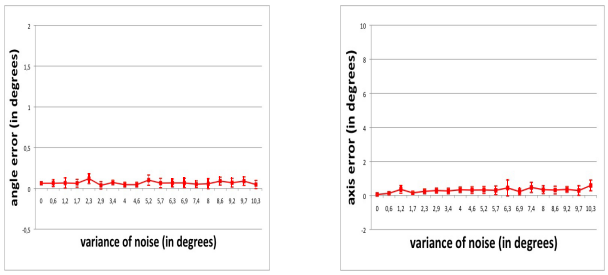

(a) Angle error. (b) Axis error.

Figure 7: Results under noise in normals.

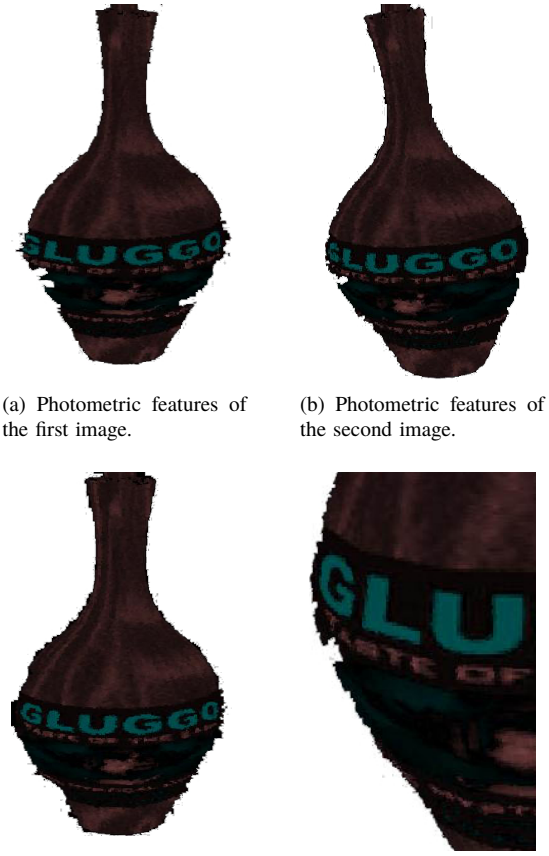

(a) Photometric features of the first image. (b) Photometric features of the second image.

(c) Result with our method. (d) Zoom into border of range images.

Figure 8: The photometric features and the result.

(a) First range image. (b) Second range image. (c) Superimposed ranged images.

Figure 9: Simulation with two light sources.

(a) Diffuse reflection model. (b) Our method.

Figure 10: Results obtained with the diffuse reflection model and with our method.

serve that the largest error remains under 1.0 degree for the angle accuracy and under 4 degrees for the axis accuracy. Figs. 9, 10 and 11 illustrate the results obtained with our method when using two light sources. We show for comparison, results obtain with the method proposed in [17]. The result obtained with the method proposed in [17] has an angle error of 4.47 degrees and an axis error of 8 degrees. In contrast our method obtained accurate result, with an angle error of 0.26 degrees and an axis error of 0.84 degrees. We observe that the diffuse reflection model is useless to obtain photometric features invariant to the pose, the viewpoint or illumination conditions while our method effectively extracts photometric features invariant to the pose, the viewpoint and the illumination conditions. The ratio of ambiguous points was of 0.285 in this experiment.

8 Conclusion

We proposed a technique for the registration of range images of a specular object devoid of salient geometric features under unknown complex illumination. By using geometric information and illumination consistency, we effectively estimate photometric properties for each light source that have significant effects in the scene. These photometric properties are invariant to the illumination or pose changes. In order to handle the case of multiple light sources, we ex-

Table 2: Results obtained with two light sources.

d	Angle error	Variance of angle error	Axis error	Variance of axis error	Ratio	Variance of ratio
1.8	0.307 degrees	0.073 degrees	0.816 degrees	0.389 degrees	0.501	0.007
1.2	0.343 degrees	0.347 degrees	2.07 degrees	1.95 degrees	0.502	0.335
0.8	0.427 degrees	0.415 degrees	1.767 degrees	1.64 degrees	0.392	0.39

(a) Albedo estimated with diffuse reflection model.

(b) Albedo in non-ambiguous regions.

(c) Albedo after extrapolation.

Figure 11: Estimated albedo maps.

trapolate reliable albedo estimates onto ambiguous regions. A robust approach for range image registration is then used to estimate the transformation aligning two range images. Experiments using synthetic data confirm the flexibility, the robustness and the accuracy of our proposed method.

References

[1] H. Bay, A. Ess, T. Tuytelaars, and L.V. Gool. Speeded-up robust features (surf). *CVIU'08*, 110(3):346–359, 2008.

[2] P. J. Besl and N. D. McKay. A method for registration of 3-D shapes. *IEEE Trans. on PAMI*, 14(2):239–256, 1992.

[3] N. Brusco, M. Andreetto, A. Giorgi, and G. M. Cortelazzo. 3D registration by textured spin-images. *In Proc. of 3DIM'05*, pages 262–269, 2005.

[4] L. Cerman, A. Sugimoto, and I. Shimizu. 3D shape registration with estimating illumination and photometric properties of a convex object. *In Proc. of CVWW'07*, pages 76–81, 2007.

[5] Guy Godin, Denis Laurendeau, and Robert Bergevin. A method for the registration of attributed range images. *In Proc. of 3DIM'01*, pages 179–186, 2001.

[6] A. E. Johnson and S. B. Kang. Registration and integration of textured 3D data. *Image and vision computing*, 17(2):135–147, 1999.

[7] T.M Lehman and C. Palm. Color line search for illuminant estimation in real-world scene. *In J.Optics Soc.*, 18(11):2679–2691, 2001.

[8] S. Lin, Y. Li, S.B. Kang, X. Tong, and H.Y Shum. Diffuse-specular separation and depth recovery from image sequences. *In Proc. of ECCV'02*, pages 210–224, 2002.

[9] Y. Liu, h. Zhou, X. Su, M. Ni, and R. J.Lloyd. Transforming least squares to weighted least squares for accurate range image registration. *In Proc. of 3DPVT'06*, pages 232–239, 2006.

[10] S.K. Nayar, X.S. Fang, and T. Boult. Separation of reflection components using color and polarization. *Int'l J. Computer Vision*, 21(3), 1996.

[11] S.K. Nayar, K. Ikeuchi, and T. Kanade. Surface reflection: Physical and geometrical perspectives. *Trans on PAMI'91*, 13(7):611–634, 1991.

[12] Okatani, I.S., and A. Sugimoto. Registration of range images that preserves local surface structures and color. *In Proc. of 3DPVT'04*, pages 786–796, 2004.

[13] K. Pulli, S. Piiroinen, T. Duchamp, and W. Stuetzle. Projective surface matching of colored 3D scans. *In Proc. of 3DIMŠ05*, pages 531–538, 2005.

[14] Y. Sato and K. Ikeuchi. Temporal-color space analysis of reflection. *J. Optics Soc. Am. A*, 11, 1994.

[15] R.T. Tan and K. Ikeuchi. Separating reflection components of textured surfaces using a single image. *IEEE Trans. on PAMI'05*, 27(2):178–193, 2005.

[16] R.T. Tan, K. Nishino, and K. Ikeuchi. Color constancy through inverse intensity chromaticity space. *J. Optics Soc. Am. A*, 21(3):321–334, 2004.

[17] D. Thomas and A. Sugimoto. Robust range image registration using local distribution of albedo. *In Proc. of 3DIM'09*, pages 1654–1661, 2009.

[18] E. Tola, V. Lepetit, and P. Fua. A fast local descriptor for dense matching. *In Proc. of CVPR'08*, pages 1–8, 2008.

[19] S. Weik. Registration of 3-D partial surface models using luminance and depth information. *In Proc. of 3DIM'97*, pages 93–101, 1997.